SUPPLEMENTAL MATERIALS AND METHODS

Preparation of ^{18}F-labeled Cycratide

For ^{18}F radiolabeling, cycratide was first conjugated with NOTA-NHS ester (CheMatech, Dijon, France). Briefly, 2 μmol of cycratide was mixed with 6 μmol of NOTA-NHS in 0.1 N $NaHCO_3$ solution (pH 9.0). After stirring at room temperature for 4 h, the NOTA-conjugated cycratide (NOTA-cycratide) was purified by semipreparative HPLC and the product was confirmed by Matrix-assisted laser desorption/ionization time-of-light mass spectrometry: *m/z* 1,140.31 for $[MH]^+$ ($C_{49}H_{85}N_{15}O_{16}$, calculated molecular weight 1,139.63 Da).

NOTA-cycratide was then labeled with ^{18}F via NOTA-Al^{18}F chelation. Briefly, No-carrier-added $^{18}F^-$ (0.74–1.48 GBq) was mixed with 24 nmol $AlCl_3$ in 100 μL sodium acetate buffer (0.1 M, pH 4.0) for 5 min at room temperature. Subsequently, 40 nmol NOTA-cycratide was added and the mixture was heated at 110°C for 15 min. After purification with Sep-Pak C18 cartridges (Waters, Milford, MA), the product was passed through 0.22-μm Millipore filters into sterile vials for further use. The radiochemical purity of ^{18}F-cycratide was determined by analytical HPLC.

Cell Uptake of ^{68}Ga-cycratide and ^{18}F-cycratide

The integrin αvβ6-positive BxPC-3 cells were seeded into 12-well plates and incubated overnight at 37°C to allow adherence. After a brief wash with PBS, cells were incubated with ^{68}Ga-cycratide or ^{18}F-cycratide (37 kBq per well) at 37°C for 10, 20, 30, 60, 120, and 240 min. After washing six times with chilled PBS, cells were collected and cell-associated radioactivity was measured using a γ counter (Packard, Meriden, CT). The cell uptake was

expressed as the percent added dose (% AD) after decay correction. Experiments were performed 3 times with four parallel samples.

Comparison of ^{18}F-cycratide with ^{68}Ga-cycratide for Small-animal PET Imaging

For direct comparison of the PET imaging of ^{18}F-cycratide with ^{68}Ga-cycratide, each BxPC-3 tumor-bearing nude mouse (n = 4) was injected with 5.55 MBq ^{18}F-cycratide via the tail vein. At 0.5, 1, and 2 h postinjection, 10-min static PET scanning was performed using a small-animal PET/CT scanner (Siemens Medical Solutions). On the second day, the same mice were injected with 5.55 MBq ^{68}Ga-cycratide via the tail vein, and 10-min static PET imaging was performed at 0.5, 1, and 2 h postinjection using the same protocol.

Biodistribution of ^{18}F-cycratide

Female BALB/c nude mice bearing subcutaneous BxPC-3 tumors were injected with 1.85 MBq ^{18}F-cycratide to evaluate the distribution of the radiotracer in the main organs (n = 4 per group). Mice were euthanized at 0.5, 1, and 2 h postinjection, and blood, tumor, and main organs/tissues were harvested, weighed, and measured using a γ counter.

^{18}F-FDG and ^{68}Ga-cycratide PET Imaging in a Dual Tumor and Inflammation Mouse Model

For the dual BxPC-3 and inflammation mouse model, 100 μL of turpentine was injected in the left thigh muscle of the BxPC-3 tumor-bearing nude mice at 24–48 h before the PET imaging experiments. Mice (n = 3) were injected with 3.7 MBq ^{18}F-FDG via the tail vein, and 10-min static PET scans were acquired at 1 h postinjection. One day later, the same

mice were injected with 5.55 MBq ^{68}Ga-cycratide, and then PET imaging was performed at 0.5 h postinjection using a small-animal PET/CT scanner (Siemens Medical Solutions).

Supplemental Table 1. Biodistribution of ^{68}Ga-cycratide in healthy volunteers (SUV, n = 5)

Time (min)	Heart	Liver	Spleen	Lung	Kidney	Intestine	Bone marrow	Brain	Muscle	Pancreas
5	5.05 ± 1.06	2.52 ±0.70	3.34 ± 0.94	1.24 ± 0.53	13.94 ± 4.39	0.91 ± 0.28	1.36 ± 0.43	0.49 ± 0.13	0.84 ± 0.07	3.18 ± 0.96
15	2.93 ± 0.69	1.58 ± 0.43	1.99 ± 0.52	0.80 ± 0.39	8.72 ± 3.03	0.72 ± 0.17	0.81 ± 0.22	0.14 ± 0.04	0.66 ± 0.08	1.99 ± 0.66
25	2.21 ± 0.44	1.22 ± 0.30	1.49 ± 0.33	0.58 ± 0.21	6.19 ± 1.59	0.60 ± 0.22	0.64 ± 0.24	0.09 ± 0.04	0.57 ± 0.12	1.41 ± 0.55
35	1.84 ± 0.32	1.01 ± 0.27	1.26 ± 0.25	0.52 ± 0.24	5.57 ± 1.69	0.55 ± 0.20	0.57 ± 0.20	0.06 ± 0.03	0.49 ± 0.09	1.15 ± 0.31
45	1.55 ± 0.22	0.86 ± 0.17	1.00 ± 0.14	0.41 ± 0.18	4.55 ± 1.44	0.44 ± 0.30	0.56 ± 0.26	0.06 ± 0.03	0.45 ± 0.14	1.06 ± 0.33
60	1.35 ± 0.19	0.74 ± 0.14	0.95 ± 0.16	0.37 ± 0.15	4.11 ± 1.20	0.44 ± 0.20	0.55 ± 0.18	0.05 ± 0.03	0.37 ± 0.08	0.82 ± 0.26
120	0.71 ± 0.05	0.40 ± 0.08	0.55 ± 0.15	0.18 ± 0.03	2.49 ± 1.45	0.18 ± 0.14	0.33 ± 0.13	0.02 ± 0.01	0.18 ± 0.03	0.41 ± 0.14

Supplemental Table 2. Radiation-absorbed dose estimates of ^{68}Ga-cycratide in healthy volunteers (mGy/MBq; n = 5, [2 women, 3 men])

Organ	Mean	SD
Adrenals	1.57E-02	2.66E-03
Brain	2.70E-03	1.49E-03
Esophagus	8.80E-03	3.38E-03
Eyes	5.78E-03	4.58E-03
Gallbladder wall	1.10E-02	2.01E-03
Left colon	1.30E-02	1.73E-03
Small intestine	1.75E-02	7.39E-03
Stomach wall	2.24E-02	1.87E-02
Right colon	1.02E-02	2.40E-03
Rectum	2.62E-02	1.87E-02
Heart wall	2.83E-02	7.99E-03
Kidneys	7.87E-02	4.98E-02
Liver	2.14E-02	1.27E-02
Lungs	2.61E-02	1.41E-02
Ovaries*	2.25E-01	7.78E-03
Pancreas	6.93E-03	1.25E-03
Prostate**	2.32E-02	1.97E-02
Salivary glands	1.03E-02	2.37E-03
Red marrow	1.06E-02	4.37E-03
Osteogenic cells	1.52E-02	6.79E-03
Spleen	3.49E-02	2.82E-02
Testes**	1.34E-02	4.60E-03
Thymus	8.88E-03	3.16E-03
Thyroid	2.86E-02	2.25E-02
Urinary bladder wall	5.59E-01	6.40E-01
Uterus*	1.42E-01	4.95E-03
Total body	1.30E-02	1.98E-03
Effective dose (mSv/MBq)	5.49E-02	4.69E-02

Note: *, n = 2; **, n = 3.

Supplemental Table 3. Characterizations of radiotracers reported in this study.

Radiotracer	Labeling yield	Synthesis time	RCP	Metabolic stability*	Tumor uptake (0.5 h p.i.)	T/M ratio (0.5 h p.i.)
^{68}Ga-linear-pep	> 95%	~20 min	> 99%	0 %	0.94 ± 0.58 %ID/g	2.27 ± 0.71
^{68}Ga-cycratide	> 95%	~20 min	> 99%	> 95%	2.15 ± 0.46 %ID/g	3.06 ± 0.28
^{18}F-cycratide	10~20%	~40 min	> 99%	> 95%	1.64 ± 0.41 %ID/g	1.98 ± 0.82

Note: RCP, radiochemical purity; p.i., postinjection; T/M ratio, tumor-to-muscle ratio; *, Metabolic stability in the blood at 0.5 h postinjection.

SUPPLEMENTAL FIGURES AND FIGURE LEGENDS

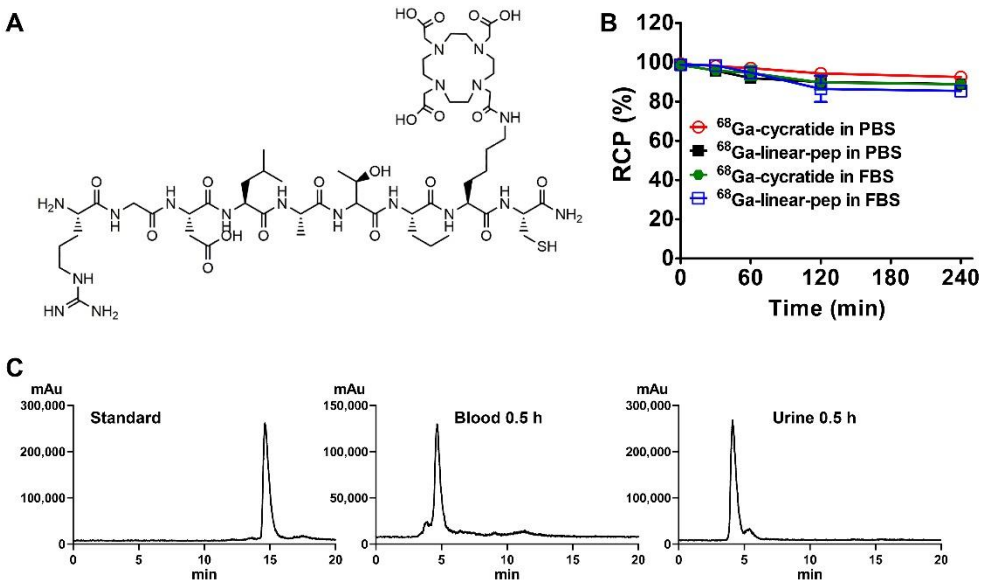

Supplemental Fig. 1. (A) Chemical structure of DOTA-linear-pep. (B) *In vitro* stability of ^{68}Ga-cycratide and ^{68}Ga-linear-pep in the fetal bovine serum (FBS) and PBS (n = 3, mean ± SD). RCP, radiochemical purity. (C) Metabolic stability of ^{68}Ga-linear-pep in the blood and urine of BALB/c mice (data are representative of three independent experiments).

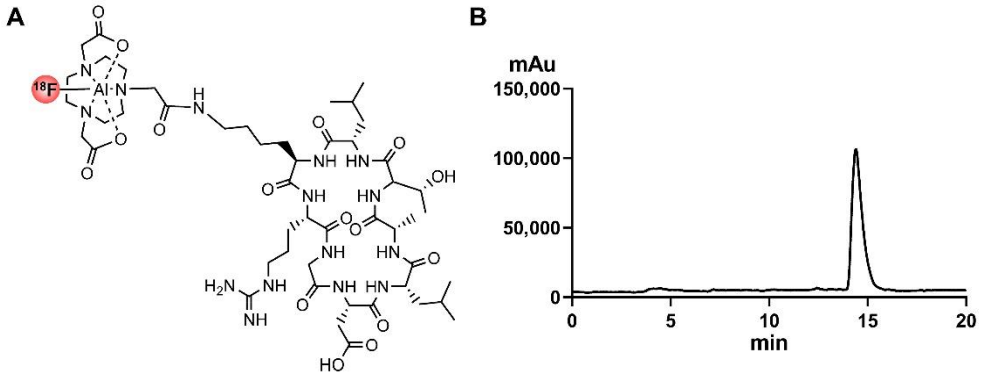

Supplemental Fig. 2. Chemical structure (A) and HPLC radiochromatogram (B) of synthesized ^{18}F-cycratide.

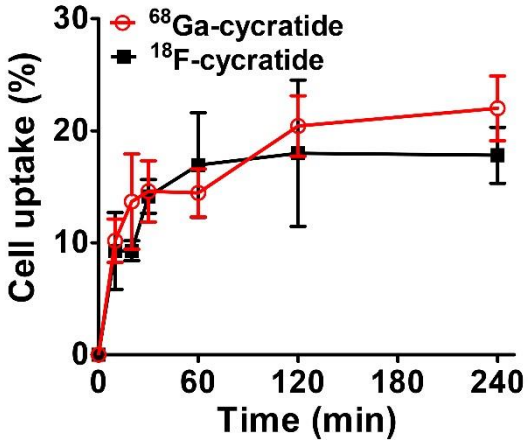

Supplemental Fig. 3. Cell uptake assay of ^{68}Ga-cycratide and ^{18}F-cycratide in BxPC-3 tumor cells (n = 4, mean ± SD).

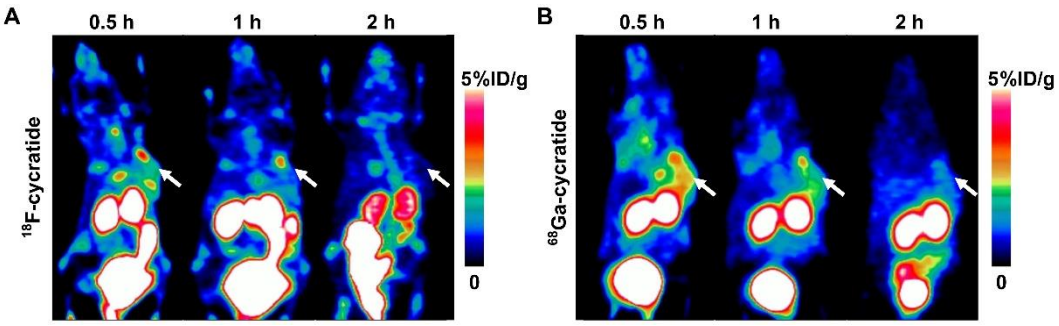

Supplemental Fig. 4. (A) Small-animal PET images obtained at 0.5, 1, and 2 h after injection of ^{18}F-cycratide in the BxPC-3 tumor-bearing BALB/c nude mice (n = 4). (B) Small-animal PET images obtained at 0.5, 1, and 2 h after injection of ^{68}Ga-cycratide in the same mice on the second day after ^{18}F-cycratide PET imaging. Tumors are indicated by arrows.

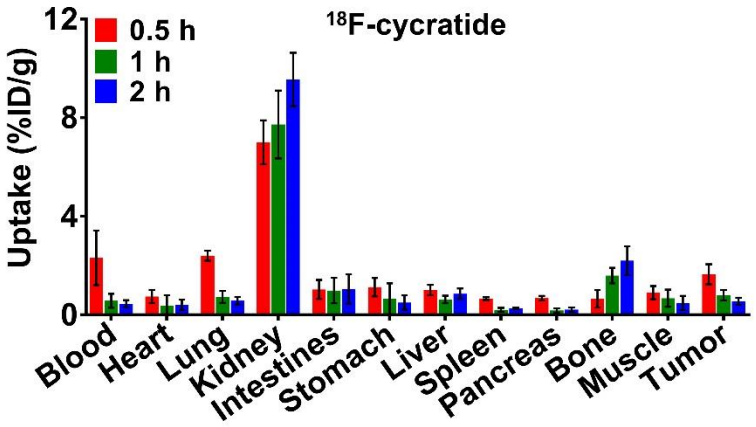

Supplemental Fig. 5. Biodistribution of ^{18}F-cycratide in BxPC-3 subcutaneous tumor-bearing BALB/c nude mice. Data are shown as mean ± SD, n = 4.

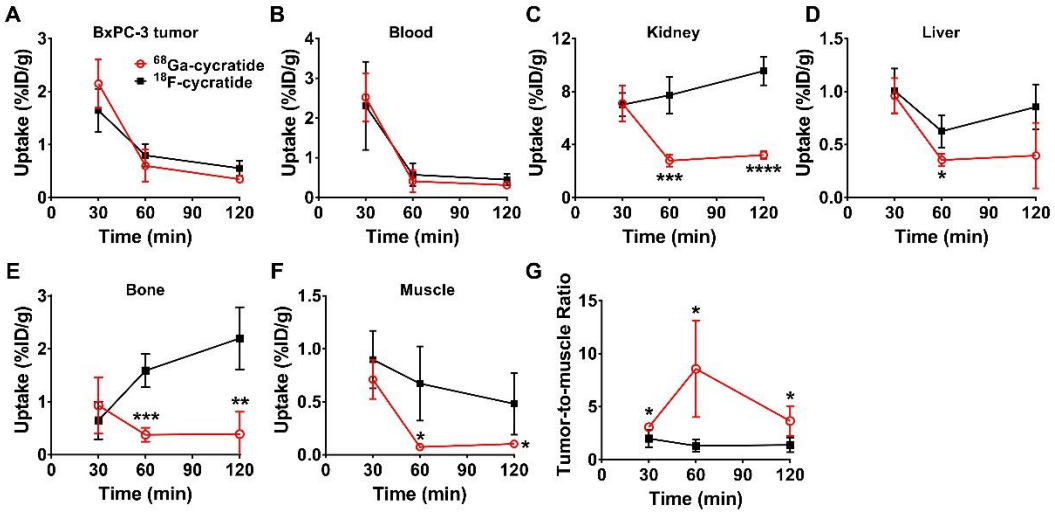

Supplemental Fig. 6. Comparison of the biodistribution of ^{18}F-cycratide and ^{68}Ga-cycratide in BxPC-3 subcutaneous tumor-bearing BALB/c nude mice. Data are shown as mean ± SD, n = 4. *, P <0.05; **, P <0.01; ***, P <0.001; ****, P <0.0001.

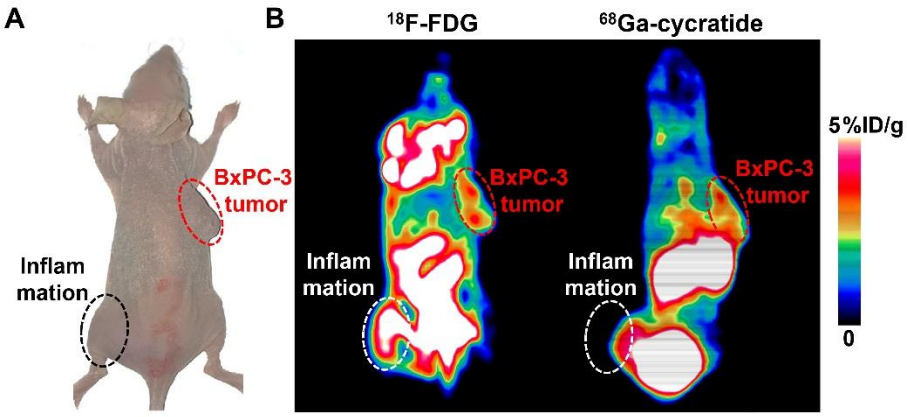

Supplemental Figure 7. PET imaging of ^{18}F-FDG and ^{68}Ga-cycratide in the dual inflammation and BxPC-3 tumor-bearing BALB/c nude mouse model (n = 3). (A) A representative of photograph of the dual inflammation and BxPC-3 tumor-bearing BALB/c nude mice. (B) Representative small-animal PET images obtained at 1 h after injection of ^{18}F-FDG and one day later at 0.5 h after injection of ^{68}Ga-cycratide in the same mouse. Tumors and inflammations are indicated by red and white dashed-line circles, respectively.